Exploring a link between the Middle Eocene Climatic Optimum and Neotethys continental arc flare-up

Annique van der Boon*[1], Klaudia F. Kuiper[2], Robin van der Ploeg[1], Margot J. Cramwinckel[1], Maryam Honarmand[3], Appy Sluijs[1], Wout Krijgsman[1]

**Corresponding author, present address: Geomagnetic Laboratory, Oliver Lodge Building, Department of Physics, Oxford Street, Liverpool, L69 7ZE, United Kingdom, AvanderBoon.work@gmail.com*

[1] Department of Earth Sciences, Utrecht University, The Netherlands; Princetonlaan 8a, 3584 CB Utrecht, The Netherlands, R.vanderPloeg@uu.nl, M.J.Cramwinckel@uu.nl, A.Sluijs@uu.nl, W.Krijgsman@uu.nl

[2]Dept. of Earth Sciences, Faculty of Science, Vrije Universiteit Amsterdam, De Boelelaan 1085, 1081 HV Amsterdam, The Netherlands, K.F.Kuiper@vu.nl

[3] Department of Earth Sciences, Institute for Advanced Studies in Basic Sciences (IASBS), P.O. Box 45195-1159, Zanjan, Iran, M.Honarmand@iasbs.ac.ir

Abstract. The Middle Eocene Climatic Optimum (MECO), a ~500 kyr episode of global warming that initiated at ~40.5 Ma, is postulated to be driven by a net increase in volcanic carbon input, but a direct source has not been identified. Here we show, based on new and previously published radiometric ages of volcanic rocks, that the interval spanning the MECO corresponds to a massive increase in continental arc volcanism in Iran and Azerbaijan. Ages of Eocene volcanic rocks in all volcanic provinces in Iran cluster around 40 Ma, very close to the peak warming phase of the MECO. Based on the spatial extent and volume of the volcanic rocks as well as the carbonaceous lithology in which they are emplaced, we estimate the total amount of CO_2 that could have been released at this time corresponds to between 1500 and 11300 Pg carbon. This is compatible with the estimated carbon release during the MECO. Although the uncertainty in both individual ages, and the spread in the compilation of ages, is larger than the duration of the MECO, a flare-up in Neotethys subduction zone volcanism represents a plausible excess carbon source responsible for MECO warming.

1 Introduction

The MECO is characterized by surface and deep ocean warming, both of approximately 2-6°C. MECO warming initiated at ~40.5 Ma, culminating in a short peak warming phase at ~40.0 Ma and terminating at ~39.9 Ma with a comparatively rapid cooling (Bijl et al., 2010; Bohaty et al., 2009; Bohaty and Zachos, 2003; Boscolo Galazzo et al., 2013, 2014; Cramwinckel et al., 2018). The MECO is associated with a rise in atmospheric CO_2 concentrations (Bijl et al., 2010; Henehan et al., 2020), extensive deep sea carbonate dissolution (Bohaty et al., 2009) and marine biotic change (Bijl et al., 2010; Cramwinckel et al., 2019; Edgar et al., 2013; Witkowski et al., 2012). The MECO inherently differs from the early Paleogene transient

warming events such as the Paleocene-Eocene Thermal Maximum (PETM; ~56 Ma) primarily in its longer duration (~500 kyr) of warming, precluding a sudden trigger but rather suggesting a continued driver (Bohaty and Zachos, 2003; Sluijs et al., 2013). Furthermore, unlike the PETM and similar transients, the MECO is not characterized by a negative $\delta^{13}C$ excursion of the exogenic carbon pool, ruling out the input of ^{13}C-depleted organic-sourced carbon as a driver, but suggesting a volcanic source (Bohaty and Zachos, 2003). Reconstructions and simulations of the carbon cycle indeed point to an imbalance in the long-term inorganic carbon cycle during the MECO (Sluijs et al., 2013), caused by enhanced volcanism and sustained by diminished continental silicate weathering (van der Ploeg et al., 2018). However, this scenario is quantitatively far from settled, partly because recent analyses based on foraminifer boron isotope ratios suggest that atmospheric CO_2 concentrations rose by significantly less than a doubling and did not rise substantially during the onset of the MECO (Henehan et al., 2020). In addition, a plausible source of excess volcanic CO_2 remains to be identified.

Here, we explore a volcanic arc flare-up in the Neotethys subduction zone as a potential source. Arc flare-ups can generate 80-90% of the total volume of igneous rocks in arc systems in periods of a few million years (Ducea and Barton, 2007). During the Eocene, a large flare-up took place in vast areas of present-day Iran (see Figure 1A) and these volcanic rocks show subduction-related geochemical signatures, representative of continental arc volcanism (Moghadam et al., 2015; Pang et al., 2013; Verdel et al., 2011). Geologic settings of the Eocene volcanic regions in Iran differ. Extensive magmatism in the Lut block is regarded by Pang et al. (2013) to be the result of post-collisional convective removal of the lithosphere and not directly related to subduction. Volcanism in the Sabzevar zone is linked by Moghadam et al. (2016) to lithospheric delamination, possibly assisted by slab-breakoff. In the Talesh/Alborz region, there are conflicting theories on the formation of the volcanic rocks. Asiabanha & Foden (2012) mention a post-collisional transition to a continental arc in their title, but then describe the volcanism as back-arc volcanism. Van der Boon (2017) gives an overview of proposed conflicting settings for volcanism in the Alborz. It is striking that in most of the areas in Iran, the flare-up is linked to an extensional setting (e.g. Verdel et al., 2011), which makes it different from other flare-ups (e.g. Ducea et al., 2015; Ducea and Barton, 2007).

The main volcanic arc associated with the Neotethys subduction zone stretches from Bazman in southeast Iran towards Azerbaijan in the northwest, from where it continues westwards into Armenia, Georgia and Turkey (van der Boon et al., 2017). North of the volcanic arc, in the Peri-Tethys basin of Azerbaijan and Russia, thick bentonites and ash layers are found within middle Eocene marine sediments (Beniamovski et al., 2003; Seidov and Alizade, 1966).

Sahandi et al. (2014) produced a compilation of geological maps of Iran, which shows that more than half of the outcrop area of igneous rocks in Iran is of Eocene age (see Figure 1A). The total surface area that is covered by Eocene igneous rocks is almost 70.000 km^2 (including units mapped as Middle Eocene, Eocene-Oligocene, etc.). A causal relationship between peak volcanism in this region and the MECO has been suggested (Allen and Armstrong, 2008; Kargaranbafghi and Neubauer, 2018), but radio-isotopic age constraints to test this hypothesis are insufficient. To quantitatively assess whether volcanism in the Iran-Azerbaijan region could have been a contributor to global warming during the MECO, we present a compilation of new and previously published radiometric ages for volcanic rocks and estimate eruptive volumes of the flare-up in Iran to evaluate how much CO_2 could have been released during this event.

2 Dating the continental arc flare-up of the Neotethys subduction zone

2.1 New $^{40}Ar/^{39}Ar$ data

We analyzed 48 samples of Eocene volcanic rocks of the Azerbaijan-Bazman Arc in Iran and Azerbaijan. Lava flows of the Peshtasar formation were dated by Vincent et al. (2005) and van der Boon et al. (2017), but ages suffered from severe excess argon. Here, we re-dated lava flows from the lower and middle part of the Peshtasar formation using new instrumentation to check for potential age bias caused by hydrocarbon interferences in previous data. We further dated samples of two ash layers in the Kura basin in Azerbaijan, as well as four volcanic rocks from the Talesh and western Alborz in Iran (see Figure 1B). Depending on the rock type, groundmass, plagioclase, sanidine, biotite and/or glass was measured (see Table 1). Thin section analysis showed pervasive alteration of volcanic rocks, disqualifying many sampled units for radio-isotope dating (see supplementary file S1 for a comparison of some thin sections). However, 8 samples showed no significant alteration and were prepared for $^{40}Ar/^{39}Ar$ dating using standard mineral separation techniques including heavy liquid and magnetic separation and handpicking. In general, fractions between 250-500 µm size were taken. For some minerals, both groundmass or glass and plagioclase or biotite could be separated.

Samples were leached with diluted HNO_3 and/or HF. Samples were irradiated during resp. 12 and 18 hours in two irradiations (VU101 in 2014 and VU107 in 2016) at the Oregon State University Triga CLICIT facility, together with Fish Canyon Tuff sanidine as standard (FCs; 28.201 ± 0.023 Ma; Kuiper et al., 2008). After irradiation samples were loaded in Cu-trays and run on a 10-collector Helix-MC mass spectrometer with an in-house built extraction with SEAS NP10, St172 and Ti sponge getters and a Lauda cooler run at -70°C, at the Vrije Universiteit Amsterdam. The used cup-configuration was either ^{40}Ar on the H2 Faraday cup and 39-36 argon isotopes on compact discrete dynodes, or both ^{40}Ar and ^{39}Ar on respectively H2 and H1 Faraday. Gain calibration was done by peakjumping CO_2 in dynamic mode on the different cups (see Monster, 2016 for details). Samples were analyzed using step-heating experiments, while for the ash layers usually single or a few grains were fused in one step and analyzed. Initial measurements were on single or a small number of grains, leading in some samples to very low intensities of ^{40}Ar (3-4 times higher than blanks). In those cases, more grains were loaded in the next experiment. Ages are calculated relative to the age of FCs reported in Kuiper et al. (2008; 28.201 ± 0.023 Ma) with decay constants of Min et al. (2000).

Out of the 8 prepared samples, 7 gave results. Our new $^{40}Ar/^{39}Ar$ ages from igneous rocks and ash layers fall within a range of ~36-45 Ma (Figure 2A), with weighted mean ages per sample between 39.3-43.1 Ma (Figure 2B). Detailed results per sample are described in supplementary file S4, and detailed results per experiment can be found in supplementary files S5-S31. Multiple aliquots of the same samples were measured. Samples of lava flows were analyzed using step-heating experiments, while for the ash layers usually single or a few grains were fused in one step and analyzed.

The integrated density distribution of these data reveals a peak at around 40.0 Ma. All compiled ages are shown together with the scaled areal extent of mapped units of Sahandi et al. (2014) (see Figure 2C).

2.2 Compilation of literature data

We combined our newly acquired data with ~370 ages from 60 published studies, including K-Ar, Ar-Ar, U-Pb, Rb-Sr and Re-Os ages (but mainly Ar-Ar and U-Pb; see supplementary file S2). Our age compilation aimed at pre-Quaternary rocks and is incomplete with respect to Quaternary volcanic rocks in Iran. We then used a kernel density plot (Vermeesch, 2012) to integrate all ages from 60-0 Ma, together with our newly acquired data. Ages and their 1σ uncertainties are used as input in the calculation of these distributions. Optimal bandwidth is calculated automatically, and we have set the bin width to 1 Myr. When studies did not report the significance level of their uncertainties, we assumed a 1σ uncertainty. Where possible, Ar-Ar ages were recalibrated to the standard of the Fish Canyon Tuff according to the Kuiper et al. (2008) calibration model. In some cases, original studies did not provide sufficient information for recalibration and then the original ages were used. All details of literature ages and associated references are added in supplementary files S2 and S3.

The compilation of $^{40}Ar/^{39}Ar$ ages from the literature, mostly from extrusive rocks (only 5 Ar-Ar ages are from intrusive rocks), yields a highly similar age density distribution to our dated samples (see Figure 3A), showing a peak at 39.7 Ma. Published U-Pb ages are typically obtained from zircons which provide less accuracy for eruption ages than $^{40}Ar/^{39}Ar$ ages from groundmass, plagioclase, sanidine or biotite (Simon et al., 2008), which is reflected in the greater width of the peaks from extrusive U-Pb ages (see Figure 3B). Combined, the Ar-Ar and U-Pb ages obtained from extrusive rocks record a 39.7 Ma peak, along with another sub-peak at 42.8 Ma (see Figure 3C).

3 Neotethys volcanism and the MECO

Considering that the Neotethys subduction zone has been active since the late Triassic (Arvin et al., 2007), our compilation shows a remarkable clustering of ages during the middle Eocene at ~40 Ma. Estimation of the areal extent of middle Eocene volcanic rocks is done using the shapefiles of Sahandi et al. (2014). For the Eocene, shapefiles are classified as 'Eocene', 'Eocene-Oligocene', 'Late Eocene-Oligocene', 'Middle Eocene', and 'Middle-Late Eocene'. We assumed that shapefiles specified as 'Eocene' had the same proportion of middle Eocene igneous rocks, and thus calculated an areal extent of 38223 km^2 of middle Eocene igneous rocks.

Our compilation indicates that many volcanic provinces in Iran were active simultaneously around 40 Ma (see Figure 2C), including the Azerbaijan-Bazman magmatic arc in the west, the Sabzevar zone in northeast Iran (Moghadam et al., 2015) and the Lut block in the east (Pang et al., 2013). Some of the largest volumes of middle Eocene volcanic rocks are located in the Talesh Mountains, where 4 out of 5 exposures with the largest areal extent are mapped (marked in white on Figure 1A). Almost three quarters of U-Pb ages (n=214) in Iran are derived from intrusive rocks (n=148). All ages of the intrusive rocks

together reveal a peak at ~39.8 Ma (Figure 3D), indicating that the peak of middle Eocene extrusive volcanism is also close in time to peak intrusive activity.

It is thus clear that the MECO corresponds to a phase of intense volcanism in the studied area. However, the average error (1σ) of the literature-based ages from 20-60 Ma is 585 kyr, and thus exceeds the duration of the MECO (500 kyr). Furthermore, the exact ages of the peaks in volcanic activity in Figure 2 are sensitive to the number of data points included and are thus not particularly robust – the addition of a few new data points may shift the peaks by thousands of years.

4 Volcanic CO_2 emissions in Iran and the MECO

The surface area of Iran covered by middle Eocene volcanic rocks is almost 40.000 km^2 (Sahandi et al., 2014; Table 2). These volcanic rocks were produced by numerous eruptions throughout the middle Eocene. In the Alborz and Central Iran, middle Eocene volcanic formations are reported to be very thick, with estimates ranging from 3-5 km in the Alborz Mountains (Stöcklin, 1974), to 6-12 km locally throughout nearly all of Iran (Berberian and King, 1981). More recent estimates of the thickness are 3-9 kilometers (e.g. Morley et al., 2009; Verdel et al., 2011). Extrapolating these thicknesses, this implies a total volume of extrusive middle Eocene volcanics between $1*10^5$ and $3.5*10^5$ km^3 (see Table 2) that potentially produced significant amounts of CO_2. Our estimates of CO_2 release due to middle Eocene volcanism in Iran are likely underestimates, as there is volcanism in other regions along the Neotethys subduction zone. Unfortunately, the lack of shapefiles of Eocene volcanic and intrusive rocks in Armenia and Azerbaijan, along the Lesser Caucasus Mountains (e.g. Allen and Armstrong, 2008), and plutons and volcanic rocks in Armenia (e.g. Moritz et al., 2016; Sahakyan et al., 2016), hampers calculations on additional CO_2 emissions within these regions.

Due to the absence of quantifications of the relation between the erupted volumes of volcanic rocks and emission of CO_2 in continental arcs, we make a comparison with the Deccan traps, for which this relation has been calculated.. The Deccan traps have an estimated eruptive volume of volcanic and volcaniclastic rocks of $1.3*10^6$ km^3 (Jay and Widdowson, 2008), with an associated emission $4.14*10^{17}$ mol CO_2 (Tobin et al., 2017). From different estimates of volume and related CO_2 emissions of Tobin et al. (2017), we obtain a linear relation of lava volume (in 10^6 km^3)/total CO_2 (in 10^{17} mol) ≈ 0.31 for the Deccan traps.

CO_2 degassing rates for continental arcs may be similar to (Marty and Tolstikhin, 1998), or larger than for continental flood basalts (McKenzie et al., 2016; Wignall et al., 2009). As a conservative starting point, we assume a similar volume versus emission relationship as the Deccan traps, which implies a minimum estimate for CO_2 release from middle Eocene volcanism in Iran between $0.37*10^{17}$ and $1.10*10^{17}$ mol (see Table 2), which corresponds to 438-1315 Pg C. Moreover, the amount of CO_2 released during volcanic episodes has been shown to increase substantially if eruptions occur among carbonate-rich sediments (Lee et al., 2013; Lee and Lackey, 2015). For example, CO_2 released from carbonate sediments during the emplacement of the Emeishan large igneous province in the end-Guadalupian was estimated to be 3.6-8.6 times higher than the amount of CO_2 released by volcanic outgassing alone (Ganino and Arndt, 2009). Indeed, the Eocene extrusive volcanism in Iran erupted through significant amounts of carbonate-rich rocks of Jurassic, Cretaceous, and

Paleogene age (e.g. Berberian and King, 1981). As a result, carbon release associated with the production of volcanic rocks in Iran could be much larger, potentially ranging from 1578 to 11,308 Pg C (see Table 2). This range of CO_2 emissions is compatible with the carbon cycle imbalance that drives the MECO in simple carbon cycle simulations constrained by available proxy data (roughly 2000-4000 Pg C; Henehan et al., 2020; Sluijs et al., 2013; van der Ploeg et al., 2018). Erosion has affected the entire Iranian plateau, and could have eroded away significant volumes of Eocene volcanic rocks. Morley et al. (2009) and Ballato et al. (2011) note that clasts in the Lower and Upper Red formation (Oligocene-Miocene age), which in many places overlie Eocene volcanics, are for a large part made up of eroded Eocene volcanic rocks. Original thicknesses of Eocene volcanic rocks in Iran could thus have been larger, making our CO_2 output estimate a minimum estimate.

5 Future perspectives

There are several obstacles in solidifying the link between warming during the MECO and volcanism in the Neotethys subduction zone. First of all, continental arcs are generally active for (tens of) millions of years, while the MECO has a duration of 500 kyr. Moreover, this duration is shorter than common uncertainties for radiometric ages in the Eocene, complicating the establishment of a causal relationship. This is important because a driver for the MECO requires excess CO_2 input only during the ~500 kyr spanning the MECO, and not during the time surrounding it (Sluijs et al., 2013). This is also supported by the drop in global ocean osmium isotope ratios, which is specifically associated with the MECO interval (van der Ploeg et al., 2018). Secondly, Iran is a relatively understudied area compared to other (continental) arcs. As a result of this, the amount of radiometric ages is low, with on average about 1 radiometric age for every several hundred km^2 of outcrop.

Therefore, the relation in time between the MECO and Neotethys arc flare-up calls for the development of much better age constraints of the volcanic deposits in Iran and this is certainly feasible. While most flare-ups have to be studied via their intrusive roots, as the extrusive record is removed through erosion (Ducea and Barton, 2007; de Silva et al., 2015), the extrusive record in Iran is extensive so that the ages can be mapped in high detail. Moreover, the respective roles of intrusive and extrusive rocks can be assessed to estimate the amount of volatiles of the igneous rocks, and sedimentological studies can provide minimum estimates on how much extrusive rock has been lost through erosion. This would help solve the question if CO_2 input rates across from the Neotethys flare-up were truly excessive and caused a net addition of CO_2 during the MECO.

6 Conclusions

We provide new Ar-Ar ages from volcanic rocks of the Azerbaijan-Bazman Arc in Iran and combine these with literature data to show that a flare-up of continental arc volcanism in Iran peaked about 40 Ma ago, conspicuously close to the Middle Eocene Climatic Optimum. We estimated volumes of middle Eocene volcanism in Iran to be between $1*10^5$ and $3.5*10^5$ km^3. We compared the volume of middle Eocene volcanics in Iran to that of the Deccan traps and estimate that between 438

and 1315 Pg of carbon in the shape of CO_2 was released during deposition. Taking into account the fact that all volcanism occurred in shallow marine basins and erupted in and through pre-existing carbonate-rich rocks, CO_2 release might have been between 1578 and 11308 Pg. Although the flare-up must be dated much better to establish its chronological relation with the MECO in more detail, we consider it a plausible major contributor to greenhouse warming during the MECO.

7 Supplementary materials

Examples of scans of thin sections are supplied in supplementary file S1. All details of literature ages and associated references are added in supplementary files S2 and S3. A detailed description of Ar-Ar results per sample is provided in supplementary file S4. Supplementary files S5-S31 show the results of the $^{40}Ar/^{39}Ar$ geochronology per experiment. S32 shows an extended version of the literature age plot of Figure 2C.

Author contributions: Fieldwork was undertaken by AvdB, MH and WK. AvdB, KFK and MH performed Ar-Ar dating. Data analysis was performed by AvdB, KFK, RvdP, MJC and AS. All authors contributed to scientific discussions and were involved in writing the manuscript.

Competing interests: The authors declare no competing interests.

Acknowledgements

This work was financially supported by Netherlands Organization for Scientific Research grant 865.10.011, awarded to WK, and was carried out under the program of the Netherlands Earth System Science Centre, financially supported by the Dutch Ministry of Education, Culture and Science. MLC and AS thank the Ammodo Foundation for funding unfettered research of laureate AS. AS thanks the European Research Council for Consolidator Grant 771497 (SPANC). We thank Roel van Elsas for help with Ar-Ar sample preparation.

References

Allen, M. B. and Armstrong, H. A.: Arabia – Eurasia collision and the forcing of mid-Cenozoic global cooling, Palaeogeogr. Palaeoclimatol. Palaeoecol., 265(1–2), 52–58, doi:10.1016/j.palaeo.2008.04.021, 2008.

Arvin, M., Pan, Y., Dargahi, S., Malekizadeh, A. and Babaei, A.: Petrochemistry of the Siah-Kuh granitoid stock southwest of Kerman, Iran: Implications for initiation of Neotethys subduction, J. Asian Earth Sci., 30(3–4), 474–489, doi:10.1016/j.jseaes.2007.01.001, 2007.

Ballato, P., Uba, C. E. C. E., Landgraf, A., Strecker, M. R. M. R., Sudo, M., Stockli, D. F. D. F., Friedrich, A. and Tabatabaei, S. H. S. H.: Arabia-Eurasia continental collision: Insights from late Tertiary foreland-basin evolution in the Alborz Mountains, northern Iran, Geol. Soc. Am. Bull., 123(1–2), 106–131, doi:10.1130/B30091.1, 2011.

Beniamovski, V. N., Alekseev, A. S., Ovechkina, M. N. and Oberhänsli, H.: Middle to upper Eocene dysoxic-anoxic Kuma

Formation (northeast Peri-Tethys): Biostratigraphy and paleoenvironments, Geol. Soc. Am. Spec. Pap., 369, 95–112, 2003.

Berberian, M. and King, G. C. P.: Towards a paleogeography and tectonic evolution of Iran, Can. J. Earth Sci., 18, 210–265, 1981.

Bijl, P. K., Houben, A. J. P., Schouten, S., Bohaty, S. M., Sluijs, A., Reichart, G.-J., Damsté, J. S. S. and Brinkhuis, H.: Transient Middle Eocene Atmospheric CO2 and Temperature Variations, Science, 330, 819–821, 2010.

Bohaty, S. M. and Zachos, J. C.: Significant Southern Ocean warming event in the late middle Eocene, Geology, 31(11), 1017–1020, 2003.

Bohaty, S. M., Zachos, J. C., Florindo, F. and Delaney, M. L.: Coupled greenhouse warming and deep-sea acidification in the middle Eocene, Paleoceanography, 24, 1–16, doi:10.1029/2008PA001676, 2009.

van der Boon, A., Kuiper, K. F., Villa, G., Renema, W., Meijers, M. J. M., Langereis, C. G., Aliyeva, E. and Krijgsman, W.: Onset of Maikop sedimentation and cessation of Eocene arc volcanism in the Talysh Mountains, Azerbaijan, Geol. Soc. London, Spec. Publ., 428, 145–169, doi:10.1144/sp428.3, 2017.

Boscolo Galazzo, F., Giusberti, L., Luciani, V. and Thomas, E.: Paleoenvironmental changes during the Middle Eocene Climatic Optimum (MECO) and its aftermath: The benthic foraminiferal record from the Alano section (NE Italy), Palaeogeogr. Palaeoclimatol. Palaeoecol., 378, 22–35, doi:10.1016/j.palaeo.2013.03.018, 2013.

Boscolo Galazzo, F., Thomas, E., Pagani, M., Warren, C., Luciani, V. and Giusberti, L.: The middle Eocene climatic optimum (MECO): A multiproxy record of paleoceanographic changes in the southeast Atlantic (ODP Site 1263, Walvis Ridge), Paleoceanography, 29, 1–19, doi:10.1002/2014PA002670, 2014.

Cramwinckel, M. J., Huber, M., Kocken, I. J., Agnini, C., Bijl, P. K., Bohaty, S. M., Frieling, J., Goldner, A., Hilgen, F. J., Kip, E. L., Peterse, F., van der Ploeg, R., Röhl, U., Schouten, S. and Sluijs, A.: Synchronous tropical and polar temperature evolution in the Eocene, Nature, 559, 382–386, doi:10.1038/s41586-018-0272-2, 2018.

Cramwinckel, M. J., van der Ploeg, R., Bijl, P. K., Peterse, F., Bohaty, S. M., Röhl, U., Schouten, S., Middelburg, J. J. and Sluijs, A.: Harmful algae and export production collapse in the equatorial Atlantic during the zenith of Middle Eocene Climatic Optimum warmth, Geology, 47(3), 247–250, 2019.

Ducea, M. N. and Barton, M. D.: Igniting flare-up events in Cordilleran arcs, Geology, 35(11), 1047–1050, doi:10.1130/G23898A.1, 2007.

Ducea, M. N., Paterson, S. R. and DeCelles, P. G.: High-volume magmatic events in subduction systems, Elements, 11(2), 99–104, doi:10.2113/gselements.11.2.99, 2015.

Edgar, K. M., Bohaty, S. M., Gibbs, S. J., Sexton, P. F., Norris, R. D. and Wilson, P. A.: Symbiont “bleaching” in planktic foraminifera during the Middle Eocene Climatic Optimum, Geology, 41(1), 15–18, doi:10.1130/G33388.1, 2013.

Ganino, C. and Arndt, N. T.: Climate changes caused by degassing of sediments during the emplacement of large igneous provinces, Geology, 37(4), 323–326, doi:10.1130/G25325A.1, 2009.

Henehan, M. J., Edgar, K. M., Foster, G. L., Penman, D. E., Hull, P. M., Greenop, R., Anagnostou, E. and Pearson, P. N.: Revisiting the Middle Eocene Climatic Optimum ‘Carbon Cycle Conundrum’ with new estimates of atmospheric pCO2 from

boron isotopes, Paleoceanogr. Paleoclimatology, doi:10.1029/2019PA003713, 2020.

Jay, A. E. and Widdowson, M.: Stratigraphy, structure and volcanology of the SE Deccan continental flood basalt province: implications for eruptive extent and volumes, J. Geol. Soc. London., 165, 177–188, 2008.

Kargaranbafghi, F. and Neubauer, F.: Tectonic forcing to global cooling and aridification at the Eocene-Oligocene transition in the Iranian plateau, Glob. Planet. Change, 171, 248–254, doi:10.1016/j.gloplacha.2017.12.012, 2018.

Kuiper, K. F., Deino, A., Hilgen, F. J., Krijgsman, W., Renne, P. R. and Wijbrans, J. R.: Synchronizing rock clocks of Earth history, Science, 320(5875), 500–4, doi:10.1126/science.1154339, 2008.

Lee, C.-T. A., Shen, B., Slotnick, B. S., Liao, K., Dickens, G. R., Yokoyama, Y., Lenardic, A., Dasgupta, R., Jellinek, M., Lackey, J. S., Schneider, T. and Tice, M. M.: Continental arc – island arc fluctuations, growth of crustal carbonates, and long-term climate change, Geosphere, 9(1), 21–36, doi:10.1130/GES00822.1, 2013.

Lee, C. A. and Lackey, J. S.: Global Continental Arc Flare-ups and Their Relation to Long-Term Greenhouse Conditions, Elements, 11(2), 125–130, doi:10.2113/gselements.11.2.125, 2015.

Marty, B. and Tolstikhin, I. N.: CO2 fluxes from mid-ocean ridges, arcs and plumes, Chem. Geol., 145, 233–248, 1998.

McKenzie, N. R., Horton, B. K., Loomis, S. E., Stockli, D. F., Planavsky, N. J. and Lee, C. A.: Continental arc volcanism as the principal driver of icehouse-greenhouse variability, Science, 352(6284), 444–447, doi:10.1126/science.aad5787, 2016.

Min, K., Mundil, R., Renne, P. R. and Ludwig, K. R.: A test for systematic errors in 40 Ar/39 Ar geochronology through comparison with U/Pb analysis of a 1.1-Ga rhyolite, Geochim. Cosmochim. Acta, 64(1), 73–98, 2000.

Moghadam, H. S., Li, X.-H., Ling, X.-X., Santos, J. F., Stern, R. J., Li, Q.-L. and Ghorbani, G.: Eocene Kashmar granitoids (NE Iran): Petrogenetic constraints from U-Pb zircon geochronology and isotope geochemistry, Lithos, 216–217, 118–135, doi:10.1016/j.lithos.2014.12.012, 2015.

Monster, M.: Multi-method palaeointensity data of the geomagnetic field during the past 500 kyrs from European volcanoes, UU Dept. of Earth Sciences, Utrecht., 2016.

Moritz, R., Rezeau, H., Ovtcharova, M., Tayan, R., Melkonyan, R., Hovakimyan, S., Ramazanov, V., Selby, D., Ulianov, A., Chiaradia, M. and Putlitz, B.: Long-lived, stationary magmatism and pulsed porphyry systems during Tethyan subduction to post-collision evolution in the southernmost Lesser Caucasus, Armenia and Nakhitchevan, Gondwana Res., 37, 465–503, doi:http://dx.doi.org/10.1016/j.gr.2015.10.009, 2016.

Morley, C. K., Kongwung, B., Julapour, A. A. A., Abdolghafourian, M., Hajian, M., Waples, D., Warren, J., Otterdoom, H., Srisuriyon, K. and Kazemi, H.: Structural development of a major late Cenozoic basin and transpressional belt in central Iran: The Central Basin in the Qom-Saveh area, Geosphere, 5(4), 325–362, doi:10.1130/GES00223.1, 2009.

Pang, K.-N., Chung, S.-L., Zarrinkoub, M. H., Khatib, M. M., Mohammadi, S. S., Chiu, H.-Y., Chu, C.-H., Lee, H.-Y. and Lo, C.-H.: Eocene–Oligocene post-collisional magmatism in the Lut–Sistan region, eastern Iran: Magma genesis and tectonic implications, Lithos, 180–181, 234–251, doi:10.1016/j.lithos.2013.05.009, 2013.

van der Ploeg, R., Selby, D., Cramwinckel, M. J., Li, Y., Bohaty, S. M., Middelburg, J. J. and Sluijs, A.: Middle Eocene greenhouse warming facilitated by diminished weathering feedback, Nat. Commun., 9(1), 2877, doi:10.1038/s41467-018-

05104-9, 2018.

Sahakyan, L., Bosch, D., Sosson, M., Avagyan, A., Galoyan, G. H., Rolland, Y., Bruguier, O., Stepanyan, Z. H., Galland, B., Vardanyan, S. and Bataillon, P. E.: Geochemistry of the Eocene magmatic rocks from the Lesser Caucasus area (Armenia): evidence of a subduction geodynamic environment, Geol. Soc. London, Spec. Publ. Tecton. Evol. East. Black Sea Caucasus, 428, 2016.

Sahandi, R., Soheili, M., Sadeghi, M., Delavar, T. and Jafari Rad, A.: Compiled geological map of Iran, scale 1:1.000.000, digitally published by the Geological Survey of Iran., 2014.

Seidov, A. G. and Alizade, K. A.: The formation and mineralogy of bentonites in Azerbaijan, Clay Miner., 6, 157–166, 1966.

de Silva, S. L., Riggs, N. R. and Barth, A. P.: Quickening the pulse: Fractal tempos in continental arc magmatism, Elements, 11(2), 113–118, doi:10.2113/gselements.11.2.113, 2015.

Simon, J. I., Renne, P. R. and Mundil, R.: Implications of pre-eruptive magmatic histories of zircons for U-Pb geochronology of silicic extrusions, Earth Planet. Sci. Lett., 266(1–2), 182–194, doi:10.1016/j.epsl.2007.11.014, 2008.

Sluijs, A., Zeebe, R. E., Bijl, P. K. and Bohaty, S. M.: A middle Eocene carbon cycle conundrum, Nat. Geosci., 6(June 2013), 429–434, doi:10.1038/ngeo1807, 2013.

Stöcklin, J.: Northern Iran: Alborz Mountains, Geol. Soc. London, Spec. Publ., 4(1), 213–234, doi:10.1144/GSL.SP.2005.004.01.12, 1974.

Tobin, T. S., Bitz, C. M. and Archer, D.: Modeling climatic effects of carbon dioxide emissions from Deccan Traps volcanic eruptions around the Cretaceous – Paleogene boundary, Palaeogeogr. Palaeoclimatol. Palaeoecol., 478, 139–148, doi:10.1016/j.palaeo.2016.05.028, 2017.

Verdel, C., Wernicke, B. P., Hassanzadeh, J. and Guest, B.: A Paleogene extensional arc flare-up in Iran, Tectonics, 30, doi:10.1029/2010TC002809, 2011.

Vermeesch, P.: On the visualisation of detrital age distributions, Chem. Geol., 312–313, 190–194, doi:10.1016/j.chemgeo.2012.04.021, 2012.

Vincent, S. J., Allen, M. B., Ismail-Zadeh, A. D., Flecker, R., Foland, K. A. and Simmons, M. D.: Insights from the Talysh of Azerbaijan into the Paleogene evolution of the South Caspian region, Geol. Soc. Am. Bull., 117(11), 1513–1533, doi:10.1130/B25690.1, 2005.

Wignall, P. B., Sun, Y., Bond, D. P. G., Izon, G., Newton, R. J., Védrine, S., Widdowson, M., Ali, J. R., Lai, X., Jiang, H., Cope, H. and Bottrell, S. H.: Volcanism, Mass Extinction, and Carbon Isotope Fluctuations in the Middle Permian of China, Science, 324, 1179–1182, doi:10.1126/science.1171956, 2009.

Witkowski, J., Bohaty, S. M., McCartney, K. and Harwood, D. M.: Enhanced siliceous plankton productivity in response to middle Eocene warming at Southern Ocean ODP Sites 748 and 749, Palaeogeogr. Palaeoclimatol. Palaeoecol., 326–328, 78–94, doi:10.1016/j.palaeo.2012.02.006, 2012.

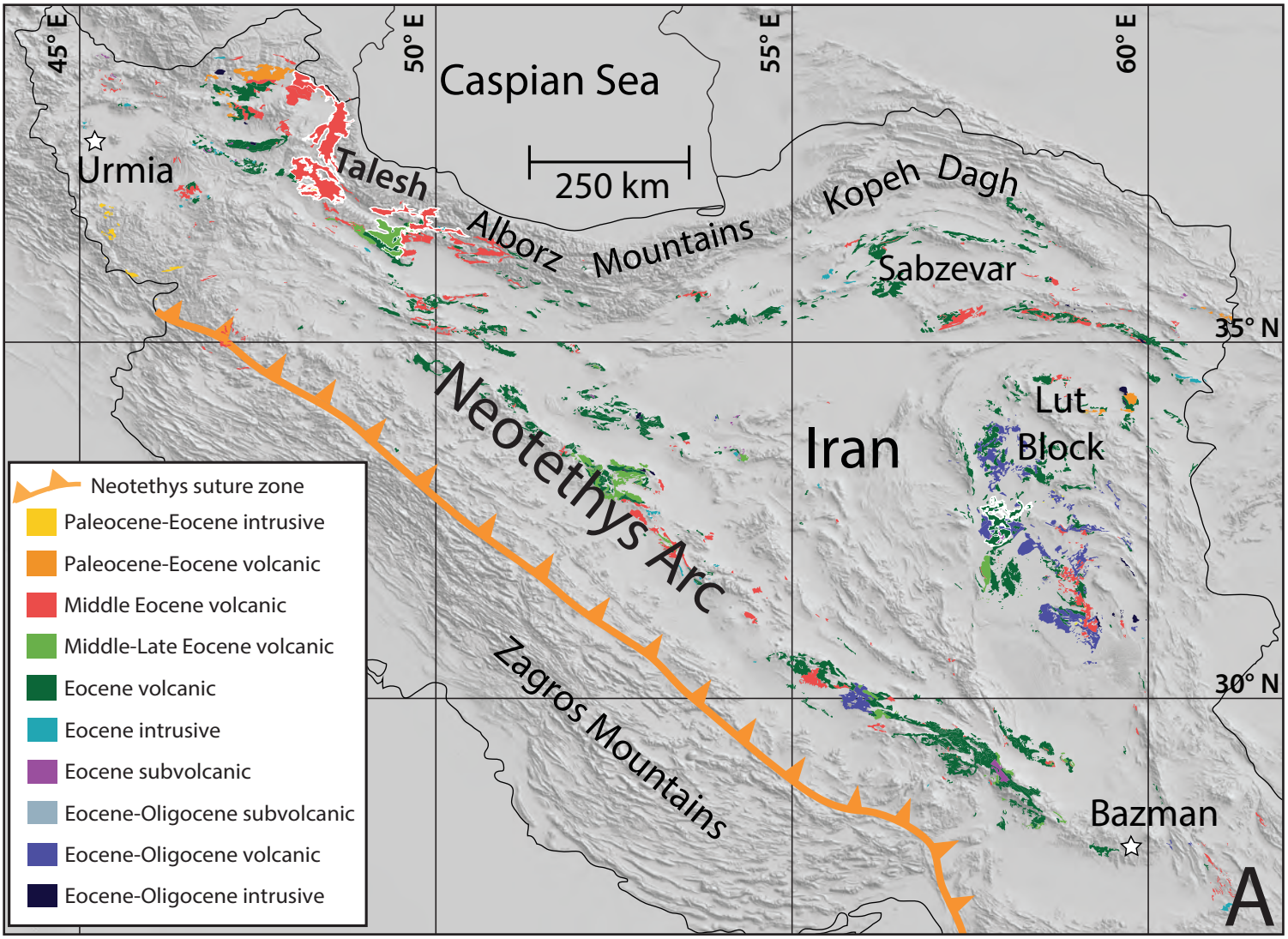

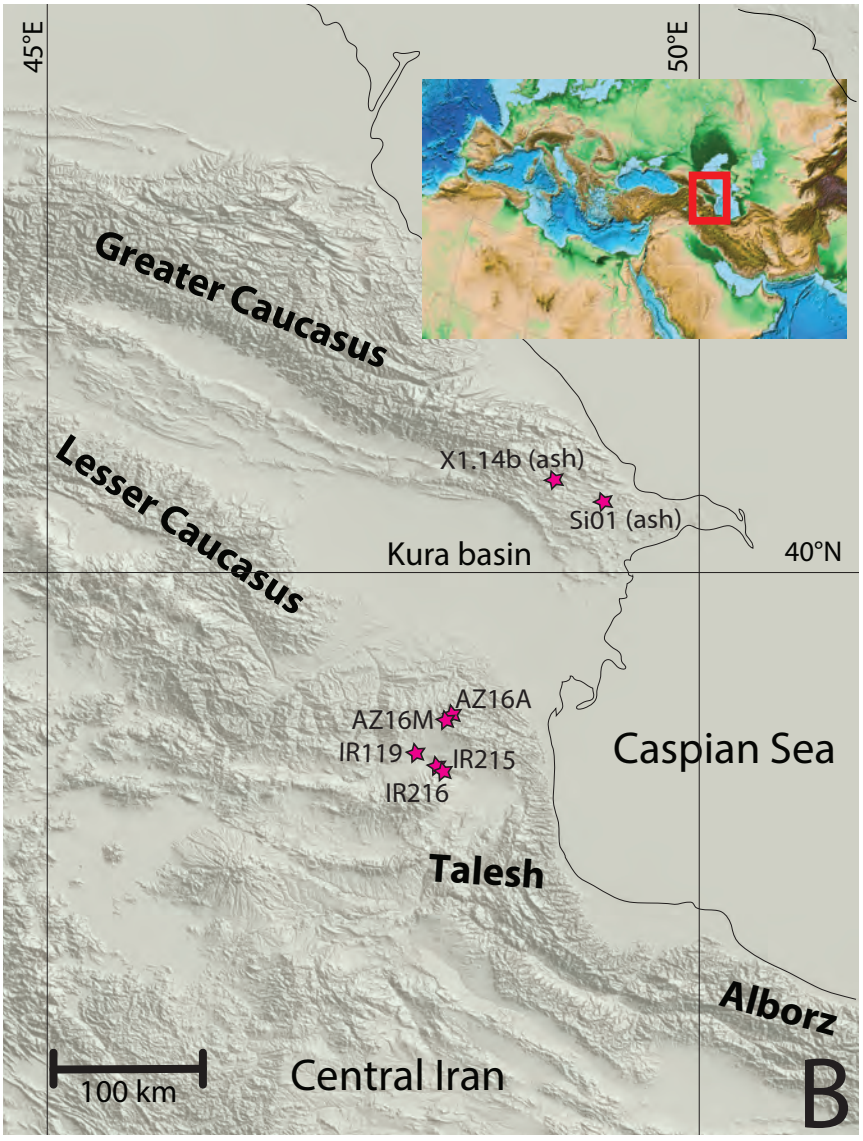

Figure 1:
A. Map showing the outcrop of Eocene volcanic rocks in Iran (modified after Agard et al., (2011) and shapefiles of Sahandi et al., (2014)). The five largest areas are shown with white outlines. **B.** Sample locations of newly acquired $^{40}Ar/^{39}Ar$ ages.

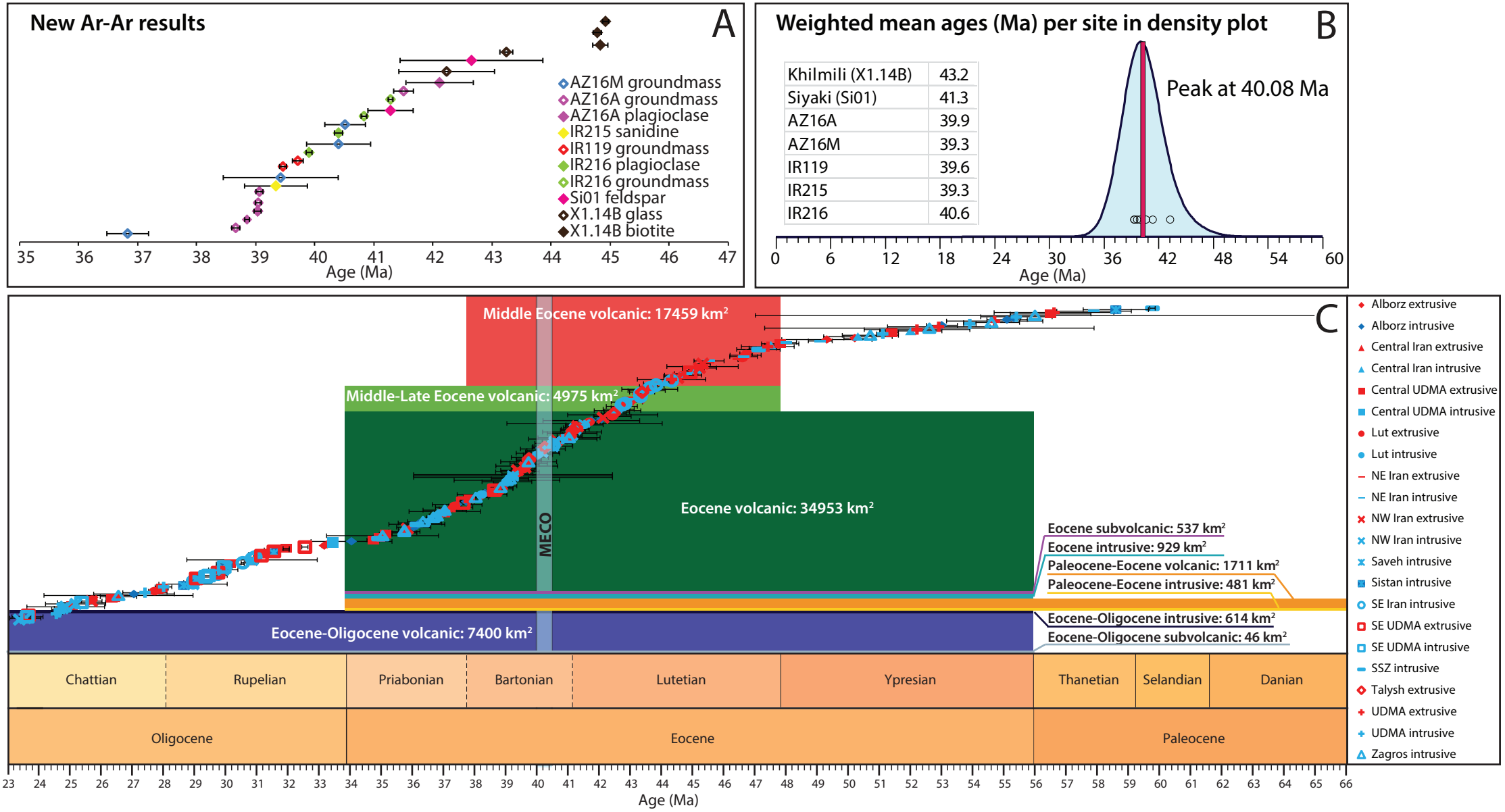

Figure 2:

A. $^{40}Ar/^{39}Ar$ dates of rocks from northwest Iran, south Azerbaijan and the Kura basin with uncertainties (1σ).

B. Kernel density plot in blue (Vermeesch, 2012) of combined $^{40}Ar/^{39}Ar$ ages. The duration and timing of the MECO event is indicated by the pink band.

C. Timescale (created with TSCreator) with scaled eruptive areas (from Sahandi et al., 2014), color legend for areas is the same as in figure 1A. Also plotted are radiometric ages from literature with associated 1σ errors, sorted by age, Y-axis is arbitrary unit. Red markers represent extrusive ages, blue markers represent intrusive ages.

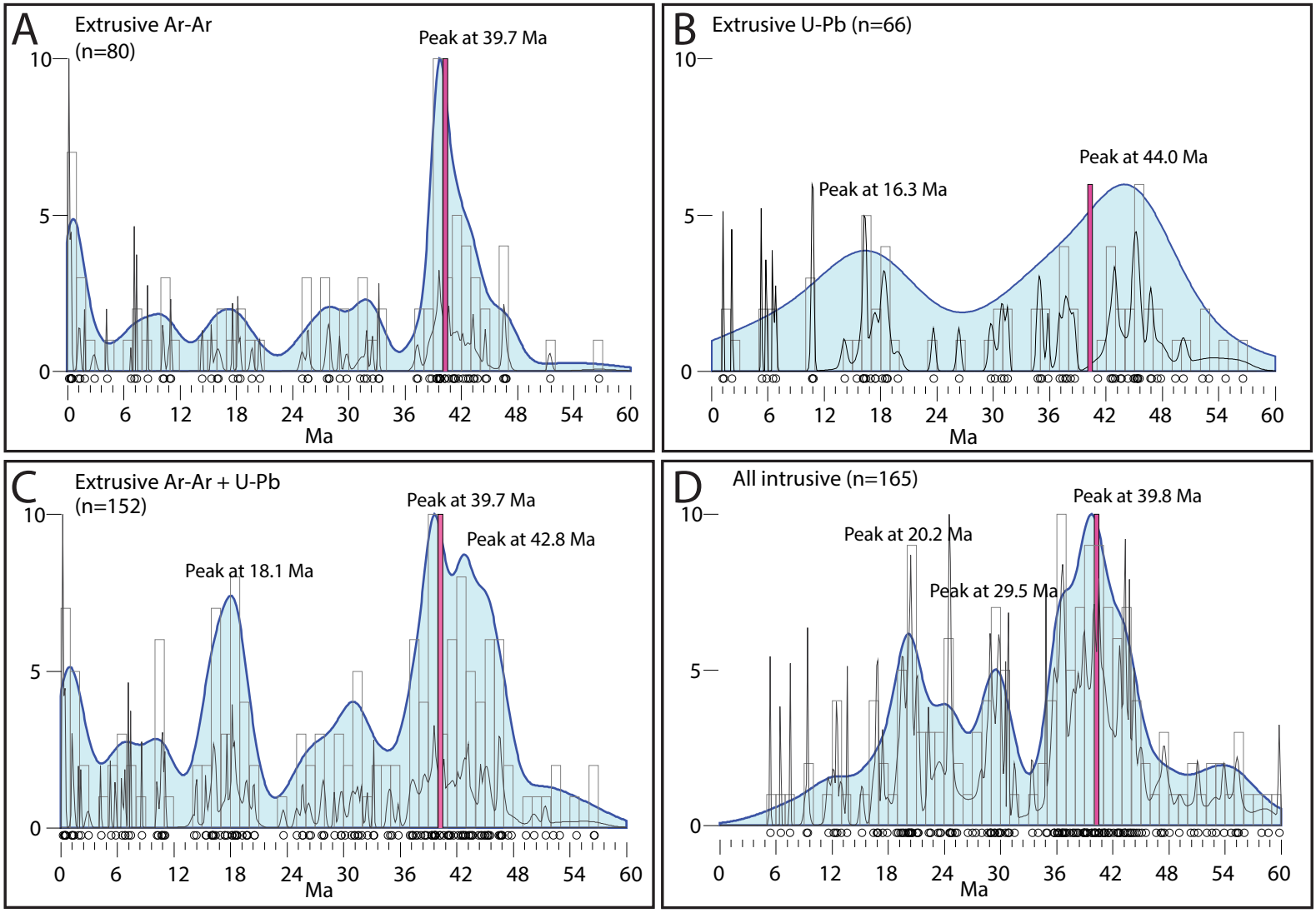

Figure 3:
Radio-isotope ages from 0-60 Ma, compiled from literature, combined with our newly obtained ages. Black thin line represents the probability density plot (PDP), blue filled line represents the kernel density estimate (KDE), boxes represent histograms (numbers on Y-axis). The timing and duration of the MECO is indicated by the pink box.

A. $^{40}Ar/^{39}Ar$ ages from literature combined with newly obtained ages for extrusive rocks only.

B. U-Pb ages from literature for extrusive rocks only.

C. $^{40}Ar/^{39}Ar$ data and U-Pb data from extrusive rocks only.

D. Combined ages from literature for intrusive rocks only.